


Article

ATSUKF-Based Actuator Health Assessment Method for Quad-Copter Unmanned Aerial Vehicles

Zhenxin Zhang , Meng Zhang *, Guoxi Li, Shilong Qin and Chunxiao Xu

College of Intelligent Science and Technology, National University of Defense Technology, Changsha 410073, China

* Correspondence: zhangmengchn@126.com or zhangmengchn@nudt.edu.cn

Abstract: The actuator, which generally consists of motors, electrical regulations, and propellers, is the key component of the quadrotor Unmanned Aerial Vehicle. During the operation of the UAV, actuators are prone to degrade performance and even cause serious failure, which affects the service quality and flight safety of Unmanned Aerial Vehicles. Therefore, timely and accurate monitoring and evaluation of the health condition of actuators is of great significance to ensure the mission reliability of UAVs. This paper proposes an Adaptive Two-stage Unscented Kalman Filter-based actuator health assessment method for Quadcopter Unmanned Aerial Vehicles. Firstly, a state space equation is established based on dynamic analysis to characterize the degradation mechanism of the actuator. Then, by modifying the Two-stage Unscented Kalman Filter algorithm, the Adaptive Two-stage Unscented Kalman Filter algorithm is constructed by combining the filter divergence criterion and the covariance matching technique to implement the health assessment of actuators. Finally, experiments are carried out for different degradation scenarios to verify the effectiveness of the proposed method.

Keywords: unmanned aerial vehicle; adaptive two-stage unscented Kalman Filter; actuators; health assessment



Citation: Zhang, Z.; Zhang, M.; Li, G.; Qin, S.; Xu, C. ATSUKF-Based Actuator Health Assessment Method for Quad-Copter Unmanned Aerial Vehicles. *Drones* **2023**, *7*, 12. <https://doi.org/10.3390/drones7010012>

Academic Editor: Andrey V. Savkin

Received: 8 December 2022

Revised: 22 December 2022

Accepted: 22 December 2022

Published: 25 December 2022



Copyright: © 2022 by the authors. Licensee MDPI, Basel, Switzerland. This article is an open access article distributed under the terms and conditions of the Creative Commons Attribution (CC BY) license (<https://creativecommons.org/licenses/by/4.0/>).

1. Introduction

In recent years, Unmanned Aerial Vehicles (UAVs) have been widely used in military operations, power inspection, agricultural plant protection, accident rescue, and other fields due to their advantages of high maneuverability, easy operation, low cost, and easy maintenance [1,2]. However, the diversity of tasks, complex external environment, and high-strength services greatly increase the failure and failure probability of key functional components, which brings a severe challenge to the safety and reliability of UAVs.

The actuator is the key component of a UAV, which consists of motors, electrical regulations, and propellers. It is an important power source for UAVs. Unfavorable factors such as long-term friction and wear, shock, and vibration exist in the service of unmanned aerial vehicles, which easily degrade the performance of actuator components, lead to control failure, and even cause serious mechanical failure. Timely and accurate monitoring and evaluation of actuator health is of great significance to ensure the normal operation and service performance of UAVs

There are two main methods for the actuator health assessment at this stage, which are the model-based health assessment method and the data-driven health assessment method. The model-based health assessment method utilizes flight state information and comprehensively considers its dynamic model to establish the corresponding physical model. However, it is difficult to build an accurate degradation process model. The data-driven health assessment method is based on the reliability of the operating state analysis by acquiring a sequence of signals from the actual operation of the actuator. However, UAV is a typical nonlinear system with various flight states and many external disturbances. It is

difficult to obtain the actuator's actual operation data directly. Therefore, the current state of health assessment of UAV actuators mostly adopts physical model-based methods, such as Kalman filters (KF), particle filters (PF) [3,4], and observers [5,6]. Many model-based robust fault diagnosis methods are summarized in [7] and [8]. These papers mainly use observers to achieve relevant functions. Although these methods can use time-domain or frequency-domain data, there are some problems such as complex modeling and no consideration of the influence of noise. The Kalman filter and its variant algorithms are common methods considering the influence of noise and its modeling process is simple. The Kalman filter and its variant algorithms reduce the model uncertainty and the effects of noise by fusing the observed and estimated data. These methods achieve actuator health assessment by comparing the differences between the system and the model. The performance degradation is usually modeled as a random model in order not to lose the sensitivity of the Kalman filter algorithm to the failure of actuator degradation [9,10]. Over the past decade, there have been some studies on health status assessment based on the Kalman filter algorithm. Zhang et al. proposed the idea of a fusion multi-Kalman filter based on interactive multi-model (IMM) estimation to estimate rotor UAV actuator failure and efficiency in [11]. Zhong et al. proposed a robust actuator fault detection and diagnosis (FDD) scheme using an adaptive three-stage Kalman filter (AThSKF) for quadcopter UAVs, which effectively reduces the impact of external interference in [12]. Gao et al. proposed an actuator FDD method based on the extended Kalman filter (EKF) and multi-model adaptive estimation (MMAE) in [13]. The actuator deflection was added to the state vector and estimated with EKF. The MMAE algorithm assigns a conditional probability to each fault actuator based on the residual of the EKF and performs fault diagnosis. Qi et al. proposed an adaptive unscented Kalman filter (AUKF) based on MIT rules to realize online estimation of UAV flight status and actuator health coefficient (AHC) in [14]. Liu et al. introduced a multi-model adaptive estimation method to monitor the health of the corresponding actuators of the UAV through a set of parallel running UKFs in [15].

Although existing methods can assess the health status of UAV actuators, they also have some limitations. Firstly, most algorithms locally linearize or linearize the UAV nonlinear system model, which results in poor numerical stability under strong non-linearity and makes it difficult to get the optimal estimate of actuator health [16]. Secondly, most of the methods that combine multi-model estimation and the Kalman filter algorithm are usually used for fault-tolerant control. They are difficult to obtain accurate health state estimation and require a relatively large amount of computation. Finally, the covariance matrix of the random walk model is mostly given according to experience. When the covariance matrix deviates from the empirical value, the effect of health state estimation will be greatly reduced or even lead to unreliable results.

Based on the relevant research results of actuator FDD, the paper takes the loss coefficient of actuator efficiency (LOE) as the standard for its health assessment. The augmented unscented Kalman filter can realize LOE estimation of actuator, but it has the problems of large amount of calculation and waste of computing resources. The TSUKF estimates the LOE of actuator based on the principle of deviation separation. Compared with the augmented unscented Kalman filter, it has the characteristics of small calculation amount and fast running speed, but it is sensitive to initial value. This paper proposes an Adaptive Two-stage Unscented Kalman Filter (ATSUKF) algorithm for the UAV nonlinear system, combining the filter divergence criterion, covariance matching technology, and Two-stage Unscented Kalman Filter (TSUKF) [9]. It is expected that this algorithm can not only estimate the status of the Rotor UAV system and LOE factors estimation of the actuators but also adaptively adjust the covariance matrix under external interference to achieve the effect of actuator health assessment.

This paper is mainly divided into five parts. Section 2 carries out system modeling for the quadcopter UAV. Section 3 describes the ATSUKF algorithm. Section 4 presents numerical simulations and results analysis. At last, the conclusions are drawn in Section 5.

2. System Modeling

2.1. Quadcopter UAV Nonlinear System Model

Physical model-based health assessment algorithm design depends on the non-linear system model. According to [16], the following assumptions are made:

- The UAV is a rigid body, which ignores the elastic vibration and deformation generated during flight.
- The inertia matrix, the gravitational acceleration and the mass are time-invariant.
- Control forces are almost always given in body-fixed frame.
- The geometric center coincides with the center of gravity.
- The effects of the ground effect are ignored.

Based on the above assumptions and [17], it can be concluded that the nonlinear dynamic equation of UAV is,

$$\begin{cases} \ddot{x} = -(\cos \psi \sin \theta \cos \phi + \sin \psi \sin \phi) \frac{u_z}{m} \\ \ddot{y} = -(\sin \psi \sin \theta \cos \phi - \cos \psi \sin \phi) \frac{u_z}{m} \\ \ddot{z} = g - (\cos \phi \cos \theta) \frac{u_z}{m} \\ \ddot{\phi} = \frac{J_{yy} - J_{zz}}{J_{xx}} \dot{\theta} \dot{\psi} + \frac{u_\phi}{J_{xx}} \\ \ddot{\theta} = \frac{J_{zz} - J_{xx}}{J_{yy}} \dot{\phi} \dot{\psi} + \frac{u_\theta}{J_{yy}} \\ \ddot{\psi} = \frac{J_{xx} - J_{yy}}{J_{zz}} \dot{\phi} \dot{\theta} + \frac{u_\psi}{J_{zz}} \end{cases} \quad (1)$$

where x , y and z is the coordinates of the center of mass of the quadrotor UAV in the inertial coordinate system, ϕ , θ and ψ are the pitch angle, roll angle, and yaw angle of the quadrotor UAV, J_{xx} , J_{yy} and J_{zz} are the inertial moments around the x , y and z axis, respectively. u_z is the total lift of the quadrotor UAV, u_ϕ , u_θ and u_ψ are the inertial moments around the ϕ , θ and ψ , respectively.

Quadcopter UAVs are mostly driven by brushless motors. Motors are controlled by the flight control system via PWM signals, which generate the torques required for the UAV flight process. The torque (τ_i) has a linear relationship with the thrust (T_i). Its relation is $\tau_i = K_\psi T_i$. The thrust generated by the motor (T_i) and the PWM control input (u_i) has a first-order linear transfer function relationship, which can be approximately expressed as $T_i = K u_i$. According to the UAV structural layout shown in Figure 1b, the relationship between lift/torque and control input is,

$$\begin{bmatrix} u_z \\ u_\phi \\ u_\theta \\ u_\psi \end{bmatrix} = \begin{bmatrix} K & K & K & K \\ -\sin(\pi/4)Kd & \sin(\pi/4)Kd & \sin(\pi/4)Kd & -\sin(\pi/4)Kd \\ \cos(\pi/4)Kd & -\cos(\pi/4)Kd & \cos(\pi/4)Kd & -\cos(\pi/4)Kd \\ KK_\psi & KK_\psi & -KK_\psi & -KK_\psi \end{bmatrix} \begin{bmatrix} u_1 \\ u_2 \\ u_3 \\ u_4 \end{bmatrix} \quad (2)$$

where d is the radius of the quadrotor UAV.

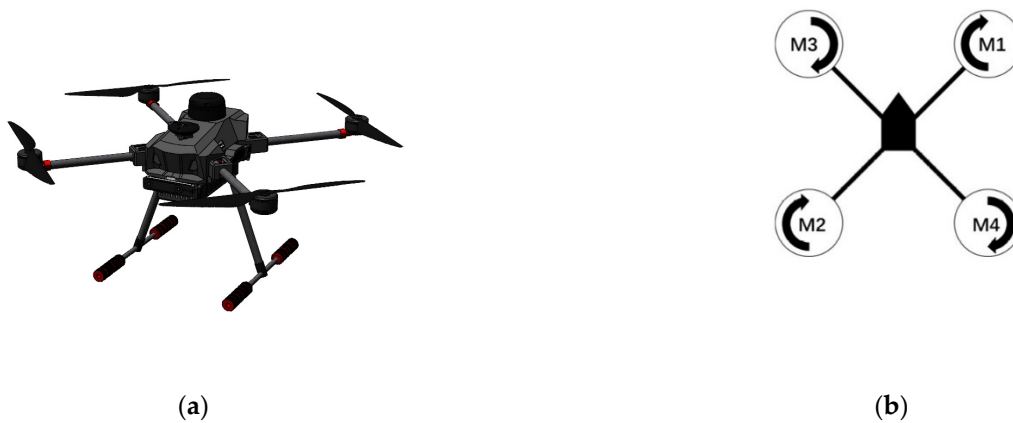


Figure 1. The UAF-02E UAV and its structure layout: (a) The UAF-02E UAV; (b) UAF-02E UAV structure layout.

2.2. Actuator Performance Degradation Model

Affected by the working environment, usage intensity, and usage habits, UAV actuators will inevitably produce slow performance degradation [11,18]. This will affect the flight safety and reliability of the UAV. Actuator degradation processes are often complex. In order to simplify the degradation process and facilitate the health assessment of actuators, this paper adopts LOE to describe the actuator performance degradation process [14].

$$u_i^\gamma = (1 - \gamma_i)u_i \quad (i = 1, 2, 3, 4) \tag{3}$$

where u_i^γ is the actual control input for the actuator; u_i is the input of the control system; γ is the LOE factor, $\gamma = 0$ indicates that the actuator has no performance degradation, $0 < \gamma < 1$ is expressed as partial performance degradation failure of the actuator, $\gamma = 1$ indicates complete failure of actuator performance.

According to [9], the actuator performance degradation model is established as a random model.

$$\begin{cases} Y_k = Y_{k-1} + \omega_{k-1}^Y \\ E(\omega_k^Y (\omega_k^Y)^T) = Q_k^Y \delta_{ij} \\ \omega_k^Y \sim N(0, Q_k^Y) \end{cases} \tag{4}$$

where Y is a constant process, driven by process noise (ω^Y); ω^Y is zero-mean Gaussian noise sequences; Q^Y is the covariance matrix of the random model; δ_{ij} is the Dirichlet function.

2.3. State Space Model

Define the state vector (x), control input vector (u), LOE vector (Y), observation vector (y_m), system noise vector (ω^x), and observation noise vector (v^x) of the UAV nonlinear system model as,

$$\begin{aligned} x &= [x \quad y \quad z \quad \phi \quad \theta \quad \psi \quad \dot{x} \quad \dot{y} \quad \dot{z} \quad \dot{\phi} \quad \dot{\theta} \quad \dot{\psi}]^T \\ u &= [u_1 \quad u_2 \quad u_3 \quad u_4]^T \\ Y &= [\gamma_1 \quad \gamma_2 \quad \gamma_3 \quad \gamma_4]^T \\ y_m &= [x \quad y \quad z \quad \phi \quad \theta \quad \psi]^T \\ \omega &= [\omega_x \quad \omega_y \quad \omega_z \quad \omega_\phi \quad \omega_\theta \quad \omega_\psi \quad \omega_{ax} \quad \omega_{ay} \quad \omega_{az} \quad \omega_{a\phi} \quad \omega_{a\theta} \quad \omega_{a\psi}]^T \\ v &= [v_x \quad v_y \quad v_z \quad v_\phi \quad v_\theta \quad v_\psi]^T \end{aligned} \tag{5}$$

According to [12] and [19], the UAV nonlinear system model can be written in the following form,

$$\begin{cases} \dot{x}(t) = f(x(t), u(t), Y(t), \omega(t)) \\ y_m(t) = h(x(t)) + v(t) \end{cases} \quad (6)$$

The noise in the system model (6) is nonlinear. For the model containing nonlinear system noise, this paper converts the nonlinear noise into additive noise by the linearization method. Its linearization method is,

$$G(t) = \frac{\partial f(x(t), u(t), Y(t), \omega(t))}{\partial \omega(t)} \quad (7)$$

$$F(t) = \frac{\partial f(x(t), u(t), Y(t), \omega(t))}{\partial Y(t)} \quad (8)$$

where $G(t)$ is the noise distribution matrix; $F(t)$ is the LOE distribution matrix. Consequently, a continuous time state space model can be obtained.

$$\begin{cases} \dot{x}(t) = f(x(t), u(t)) + F(t)Y(t) + G(t)\omega(t) \\ y(t) = h(x(t)) + v(t) \end{cases} \quad (9)$$

Kalman filter assumes that the noise of the continuous state space system model (9) follows a Gaussian distribution with zero mean. Since the method presented in this paper is based on the discrete filter design, the continuous time state space system model (9) is discretized according to the Eulerian method.

$$x(t_{k+1}) = x(t_k) + \dot{x}(t_k) \cdot \Delta t = f_d(x(t_k), u(t_k)) + F_d(t_k)Y(t_k) + G_d(t_k)\omega(t_k) \quad (10)$$

The discrete observation equation is,

$$y_{k+1} = h_{k+1}(x_{k+1}) + v_{k+1} \quad (11)$$

The system noise and measurement noise of the discrete model are defined as,

$$\omega_k = G_d(t_k)\omega(t_k) \quad (12)$$

$$v_k = v(t_{k+1}) \quad (13)$$

Because the Gaussian distribution is still a Gaussian distribution after linear transformation, the system noise in the discretized state space model still obeys the Gaussian distribution.

$$\omega_k \sim N(0, Q_k) \quad (14)$$

$$v_k \sim N(0, R_k) \quad (15)$$

Q_k is the system noise covariance matrix for a nonlinear system model; R_k is the observed noise covariance matrix for a nonlinear system model.

Thus, formula (10) can be rewritten as,

$$x_{k+1} = f_d(x_k, u_k) + F_k^r Y_k + \omega_k \quad (16)$$

where

$$F_k^r = F_d(t_k) \quad (17)$$

$$Y_k = Y(t_k) \quad (18)$$

Based on formulas (4), (11), and (18), a discrete system state space model including actuator degradation can be obtained.

$$\begin{cases} x_{k+1} = f_d(x_k, u_k) + F_k^r Y_k + \omega_k \\ Y_{k+1} = Y_k + \omega_k^Y \\ y_{k+1} = h_{k+1}(x_{k+1}) + v_{k+1} \end{cases} \quad (19)$$

3. ATSUKF-Based Actuator Health Assessment Algorithm

3.1. TSUKF-Based Algorithm

The key technology of UKF is the unscented transformation (UT), which approximates the probability density distribution of the system’s nonlinear function by constructing a set of determined sigma points to solve the non-linear filtering problem [11]. Compared with KF and EKF, the UKF can directly use the system model and avoid the error caused by linearization [20]. In order to solve the problem of inaccurate LOE factor estimation of the actuator, the idea of UKF is applied to the TSKF algorithm, and the TSUKF algorithm is formed. The TSUKF algorithm runs an unbiased state filter and a biased state filter in parallel. The final state and fault estimates are obtained by fusing the estimates of the two filters through a coupling matrix [21]. The working process of the algorithm is shown in Figure 2.

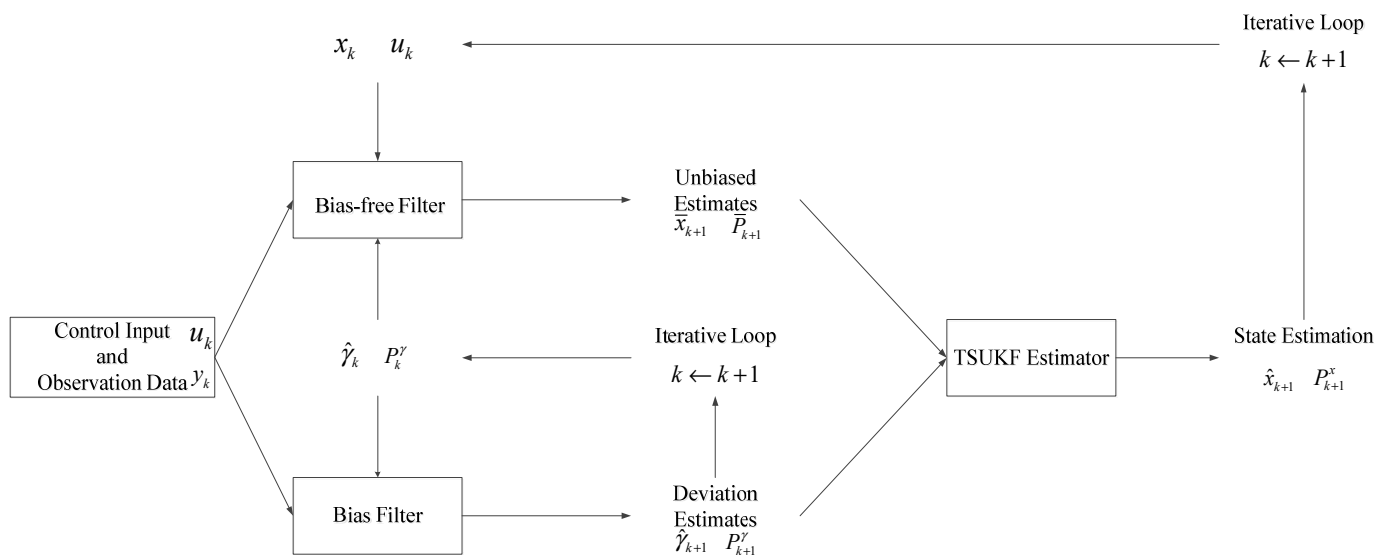


Figure 2. The working process of TSUKF.

According to [22], when the nonlinear discrete-time stochastic system model is given by (18), a discrete-time TSUKF is given by the following coupled difference equations.

$$\hat{x}_{k+1} = \bar{x}_{k+1} + \beta_{k+1} \hat{\gamma}_{k+1} \quad (20)$$

$$P_{k+1}^x = \bar{P}_{k+1} + \beta_{k+1} P_{k+1}^\gamma \beta_{k+1}^T \quad (21)$$

The bias-free filter is,

$$\chi_{k+1|k}^i = f_d(\chi_k^i) + r_k \gamma_{k|k} - \beta_{k+1|k} \gamma_{k|k} \quad i = 0, 1, \dots, 2n \quad (22)$$

$$\tilde{x}_{k+1|k} = \sum_{i=0}^{2n} w_i^m \chi_{k+1|k}^i \quad (23)$$

$$\bar{P}_{k+1|k} = \sum_{i=0}^{2n} w_i^c (\chi_{k+1|k}^i - \tilde{x}_{k+1|k}) (\chi_{k+1|k}^i - \tilde{x}_{k+1|k})^T - \beta_{k+1|k} P_{k+1|k}^\gamma \beta_{k+1|k}^T + r_k P_k^\gamma r_k^T + Q_k \quad (24)$$

$$y_{k+1|k}^i = h(\chi_{k+1|k}^i) \quad i = 0, 1, \dots, 2n \tag{25}$$

$$\tilde{y}_{k+1|k} = \sum_{i=0}^{2n} w_i^m y_{k+1|k}^i \tag{26}$$

$$\bar{P}_{k+1|k}^{yy} = \sum_{i=0}^{2n} w_i^c (y_{k+1|k}^i - \tilde{y}_{k+1|k}) (y_{k+1|k}^i - \tilde{y}_{k+1|k})^T + R \tag{27}$$

$$\bar{P}_{k+1|k}^{xy} = \sum_{i=0}^{2n} w_i^c (\chi_{k+1|k}^i - \tilde{x}_{k+1|k}) (y_{k+1|k}^i - \tilde{y}_{k+1|k})^T \tag{28}$$

$$K_{k+1}^x = \bar{P}_{k+1|k}^{xy} (\bar{P}_{k+1|k}^{yy})^{-1} \tag{29}$$

$$\bar{x}_{k+1} = \bar{x}_{k+1|k} + K_{k+1}^x (y_{k+1} - \tilde{y}_{k+1|k}) \tag{30}$$

$$\bar{P}_{k+1} = \tilde{P}_{k+1|k} - K_{k+1}^x \bar{P}_{k+1|k}^{yy} (K_{k+1}^x)^T \tag{31}$$

The bias filter is,

$$\hat{\gamma}_{k+1|k} = \hat{\gamma}_k \tag{32}$$

$$P_{k+1|k}^\gamma = P_k^\gamma + Q_k^\gamma \tag{33}$$

$$K_{k+1}^\gamma = P_{k+1|k}^\gamma H_{k+1|k}^T (\bar{P}_{k+1|k}^{yy} + H_{k+1|k} P_{k+1|k}^\gamma H_{k+1|k}^T)^{-1} \tag{34}$$

$$\hat{\gamma}_{k+1} = \hat{\gamma}_{k+1|k} + K_{k+1}^\gamma (y_{k+1} - H_{k+1}^\gamma \bar{x}_{k+1|k} - H_{k+1|k} \hat{\gamma}_{k+1|k}) \tag{35}$$

$$P_{k+1}^\gamma = P_{k+1|k}^\gamma - K_{k+1}^\gamma P_{k+1|k}^{yy} (K_{k+1}^\gamma)^T \tag{36}$$

and the coupling equations are,

$$r_k = F_k^x \beta_k + F_k^r \tag{37}$$

$$H_{k+1|k} = H_k^x \beta_{k+1|k} \tag{38}$$

$$\beta_{k+1|k} = r_k P_k^\gamma (P_{k+1|k}^\gamma)^{-1} \tag{39}$$

$$\beta_{k+1} = \beta_{k+1|k} - K_{k+1}^x H_{k+1|k} \tag{40}$$

and

$$F_k^x = \frac{1}{2\sqrt{n+\lambda}} \cdot \left\{ \sum_{i=1}^n [\chi_{k+1|k}^i - \chi_{k+1|k}^{i+n}] e_i^T \right\} (\sqrt{P_k^x})^{-1} \tag{41}$$

$$H_k^x = \frac{1}{2\sqrt{n+\lambda}} \cdot \left\{ \sum_{i=1}^n [y_{k|k-1}^i - y_{k|k-1}^{i+n}] e_i^T \right\} (\sqrt{\bar{P}_{k+1|k}})^{-1} \tag{42}$$

where the element i of $e_i \in R^n$ is 1, other elements are 0. The sample points (χ_k^i) and the corresponding coefficients w_i^m and w_i^c are expressed as.

$$\begin{cases} \chi_k^0 = x_k \\ \chi_k^i = \chi_k^0 + \left(\sqrt{(n+\lambda)P_k^i} \right), & i = 1, 2, \dots, n \\ \chi_k^i = \chi_k^0 - \left(\sqrt{(n+\lambda)P_k^i} \right), & i = n+1, n+2, \dots, 2n \end{cases} \tag{43}$$

$$\begin{cases} w_0^m = \frac{\lambda}{n+\lambda} \\ w_0^c = \frac{\lambda}{n+\lambda} + (1 - \alpha^2 + \beta) \\ w_i^m = w_i^c = \frac{1}{2(n+\lambda)}, & i = 1, 2, \dots, 2n \end{cases} \tag{44}$$

where w_i^m and w_i^c are the weighted values of the Sigma point mean and covariance, respectively; n is the dimension of the state vector (x); $\lambda = \alpha^2(n + \kappa) - n$ is the conversion factor; α determines the probability distribution of sigma points and the value range is $10^{-4} \leq \alpha \leq 1$; β is related to the form of the parametric distribution and usually takes the value of 2 when β is for a Gaussian distribution; κ usually takes the value of $3 - n$.

3.2. ATSUKF-Based Algorithm

TSUKF algorithm can estimate the LOE factor of the UAV actuator, but the selection of statistical parameters has a great influence on the accuracy and speed of parameter estimation. When the system model parameters are accurate, the norm of the predictive error covariance will gradually decrease during filtering, and the correction effect of real-time observation on the state estimation will be weakened. Under the condition of an inaccurate system model and internal and external interference, the covariance of the measured noise may be nonpositive and the filtering is easy to diverge. The random model has a great influence on the estimation accuracy of TSUKF. The value of the diagonal elements of the random model covariance matrix reflects the rate of change of the LOE factor. The larger the value of the diagonal element, the faster the LOE factor changes. The covariance matrix also reflects the linear correlation of different actuator degradation states. The covariance matrix of the random model is usually given as a constant value matrix according to the designer's experience, which is difficult to match with the dynamic characteristics of the actual degradation [23]. Therefore, this section constructs an ATSUKF algorithm for the covariance matrix (Q^Y) of the online adaptive random model according to the filter divergence criteria and covariance matching technology [24,25].

The system model used by ATSUKF is the same as that of TSUKF, and the basic filter is also the same as that of TSUKF. The criterion of filter divergence is used as the judgment basis for adaptive adjustment of the covariance matrix (Q^Y). The criterion for judging filter divergence is,

$$\varepsilon_k^T \varepsilon_k \leq K \cdot \text{tr} \left[E \left(\varepsilon_k \varepsilon_k^T \right) \right] \tag{45}$$

where K is a variable factor, the value usually takes $K \geq 1$. The larger the value of K , the looser the judgment condition. $\text{tr}[\cdot]$ is to find the trace of the matrix. When the formula (50) is established, the filtering algorithm is stable, and the ATSUKF algorithm degenerates into the TSUKF algorithm; when the formula (50) is not established, the filtering algorithm has a divergent trend, and an adaptive factor (δ_k) needs to be introduced to adjust the covariance matrix (Q^Y) to improve the correction effect of observations on the algorithm.

According to [23], the system noise covariance matrix of the random walk model is expressed as,

$$P_{k+1|k}^{\gamma yy} = \bar{P}_{k+1|k}^{\gamma yy} + H_{k+1|k} P_{k+1|k}^{\gamma} H_{k+1|k}^T \tag{46}$$

At the same time, according to the actual measured data, it can be obtained.

$$\bar{P}_{k+1|k}^{\gamma yy} = \frac{1}{M-1} \sum_{i=k-M+1}^k \varepsilon_i^{\gamma} \varepsilon_i^{\gamma T} \tag{47}$$

and

$$\varepsilon_i^{\gamma} = y_i - h \left(\bar{x}_{i|i-1} \right) - H_{i|i-1} Y_{i|i-1} \tag{48}$$

where ε_i^{γ} is the residual of the biased state filter; M is the size of the moving window, indicating the amount of historical data used by the adaptive factor, which is a finite value.

In the case of external interference and low model accuracy, the theoretical and estimated residual covariance values usually satisfy,

$$\bar{P}_{k+1|k}^{\gamma yy} \geq P_{k+1|k}^{\gamma yy} \tag{49}$$

This section introduces an adaptive factor (δ_k) to adjust the covariance matrix (Q^Y). Formulas (32), (46), and (47) are brought into formula (49) to show.

$$\frac{1}{M-1} \sum_{i=k-M+1}^k \varepsilon_i^\gamma \varepsilon_i^{\gamma T} = \bar{P}_{k+1|k}^{yy} + H_{k+1|k} (P_k^\gamma + \delta_k Q_k^\gamma) H_{k+1|k}^T \quad (50)$$

where the adaptation factor (δ_k) can be determined by,

$$\delta_k = \begin{cases} \delta_0, & \delta_0 \geq 1 \\ 1, & \delta_0 < 1 \end{cases} \quad (51)$$

$$\delta_0 = \frac{\text{tr} \left(\frac{1}{M-1} \sum_{i=k-M+1}^k \varepsilon_i^\gamma \varepsilon_i^{\gamma T} - \bar{P}_{k+1|k}^{yy} - H_{k+1|k} P_k^\gamma H_{k+1|k}^T \right)}{\text{tr} \left(H_{k+1|k} Q_k^\gamma H_{k+1|k}^T \right)} \quad (52)$$

In this section, the TSUKF algorithm is extended to the ATSUKF algorithm by introducing the adaptive factor (δ_k) to realize the adaptation of the covariance matrix (Q^Y). The degenerate nature of the actuator creates a mismatch in the noise variance, which amplifies the covariance matrix. Judging by the criterion of filter divergence, the adaptive factor (δ_k) is calculated by using the difference between the noise variance matrix obtained from M state measurement data and the noise variance matrix transmitted by the system. M measurement data are used in the calculation process to prevent the single measurement data from influencing the system too much. When the statistical characteristics of the noise are known and the actuator degradation is unchanged, the adaptive factor is 1 and the ATSUKF algorithm is equivalent to the TSUKF algorithm, and the evaluation performance is equivalent. However, when the statistical characteristics of noise are uncertain or the degree of actuator degradation changes, the ATSUKF algorithm will have higher estimation accuracy than the TSUKF algorithm.

4. Numerical Simulations

4.1. Simulation Parameters

This section evaluates the performance of the ATSUKF-based actuator health assessment evaluation algorithm through numerical simulations. The parameters of the UAV model are shown in Table 1 [26]. In order to fully verify the effectiveness of the ATSUKF algorithm, different degradation scenarios are considered in this section. In order to verify the robustness of the ATSUKF algorithm, two cases of matching and mismatching covariance matrices in the random model are considered.

Table 1. System parameters of UAF-02E.

Parameter	Value	Unit
m	1.4	kg
g	9.8	m/s ²
J_{xx}	0.0211	kg·m ²
J_{yy}	0.0219	kg·m ²
J_{zz}	0.0366	kg·m ²
d	0.0225	m
K	11.18	N
K_ψ	0.0161	

Simulation experiments use two different sets of values to initialize the covariance matrix of the random walk model to simulate whether it matches the actual one. Simulation experiments are carried out to verify the responsibility of the algorithm for failure by injecting ramp failure and step failure.

In the simulation, the drone is in hover mode at an altitude of 1m. The ramp failure fault and step failure fault are injected in 30 to 40 s and 50 to 80 s.

The mathematical expression for injection failure is,

$$\begin{cases} F1 = 0.02 * (t - 30) \\ F2 = 0.4 \end{cases} \tag{53}$$

The initial value of the algorithm and the parameter setting of the covariance matrix during the simulation process are shown in Table 2.

Table 2. The initial value of the algorithm and the parameters of the covariance matrix.

Type	Parameter	Value
Covariance Matrix Parameters	Q_1^γ	$10^{-2}I_{4 \times 4}$
	Q_2^γ	$10^{-7}I_{4 \times 4}$
	Q_x	$diag\{10^{-5}I_{6 \times 6}, 10^{-8}I_{6 \times 6}\}$
	R	$10^{-7}I_{6 \times 6}$
Algorithm initial value	x_0	$[I_{3 \times 1}, 0_{9 \times 1}]$
	Y_0	$0_{4 \times 1}$
Algorithm initial value	P_0^x	$I_{12 \times 12}$
	P_0^γ	$10^{-6}I_{4 \times 4}$
	β_0	$O_{12 \times 4}$
	t_s	0.01
	M	150

In the simulation experiment, when the covariance matrix (Q^Y) matches the actual situation, the initial value (Q_1^γ) is assigned to $10^{-2}I_{4 \times 4}$; otherwise, the initial value (Q_2^γ) is assigned to $10^{-7}I_{4 \times 4}$. In addition, Gauss noise is added to the numerical simulation experiments to make numerical simulations more practical and verify the effectiveness of the proposed method. Its variance is 0.001

4.2. Simulation Results

4.2.1. Scenario 1: Performance Degradation of a Single Actuator

In Scenario 1, the LOE factor of motor No. 1 changes as shown in the formula (58). The simulation results are shown in Figures 3 and 4, where the solid line represents the LOE change during the simulation.

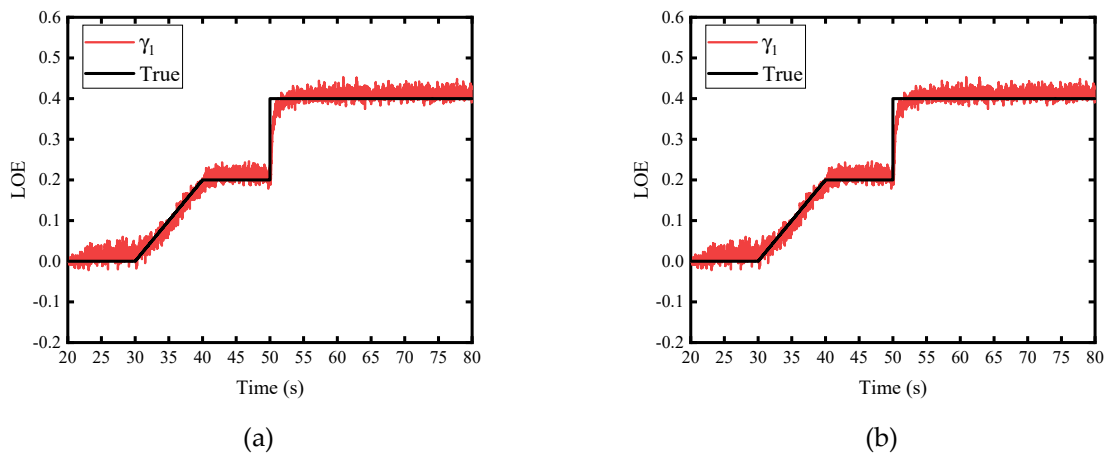


Figure 3. Simulation results when Q^Y match the actual situation in scenario 1. (a) LOE factors estimation using TSUKF; (b) LOE factors estimation using ATSUKF.

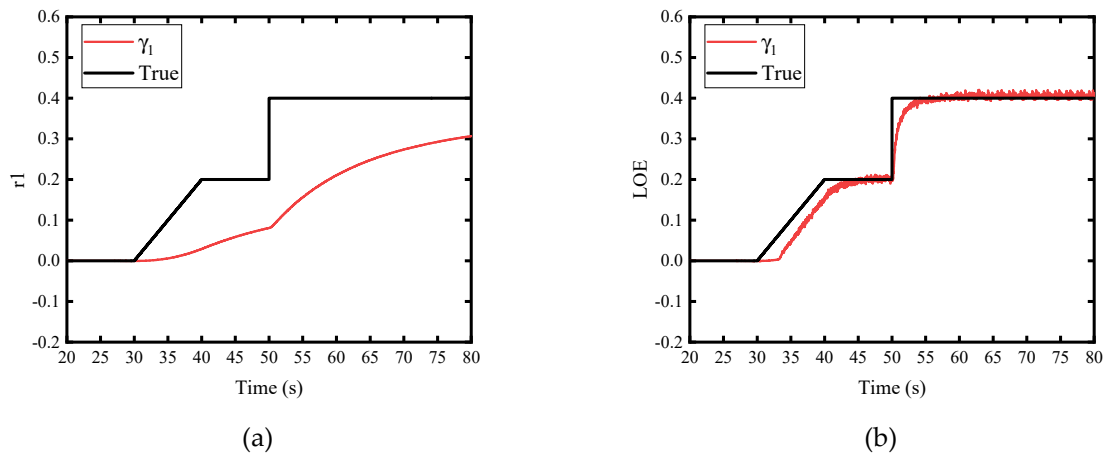


Figure 4. Simulation results when Q^Y matches the actual situation in scenario 1. (a) LOE factors estimation using TSUKF; (b) LOE factors estimation using ATSUKF.

According to Figures 3 and 4, the LOE evaluation performance of the ATSUKF algorithm is better in the case of performance degradation of a single actuator. When the covariance matrix of the random model matches, TSUKF and ATSUKF have the same accuracy. However, when the covariance matrix of the random model does not match the actual covariance matrix, the TSUKF algorithm cannot track the status of LOE factors well and almost loses the ability to estimate LOE in the process. The ATSUKF algorithm can still maintain the prediction accuracy of the random walk model

4.2.2. Scenario 2: Performance Degradation of Multiple Executors

In Scenario 2, the LOE factors of all motors change as shown in the formula (53) when hovering at the same time.

Simulation results of Condition 1 are shown in Figures 5–8.

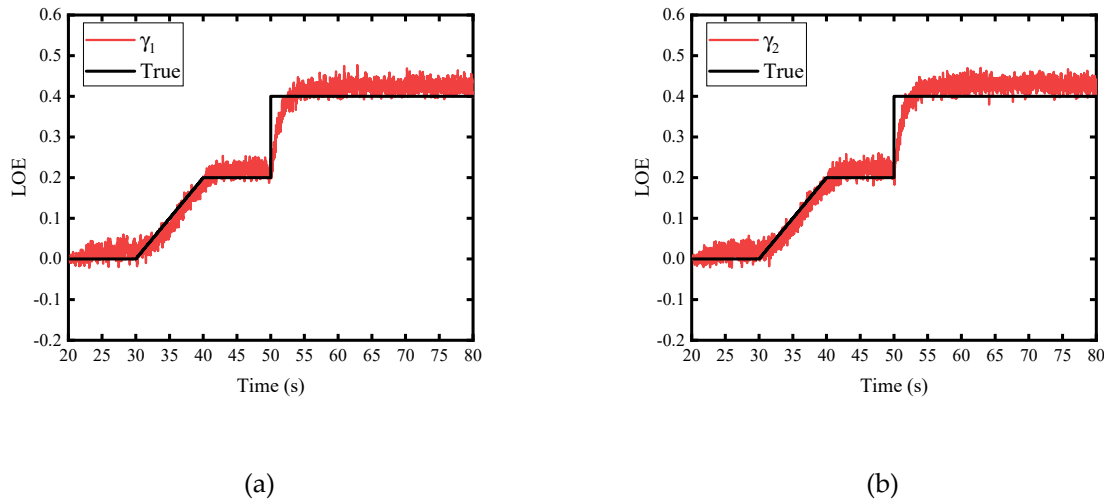
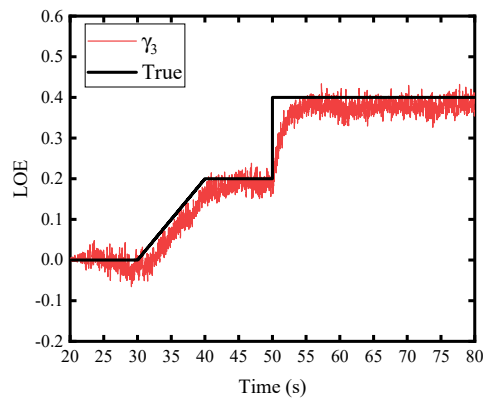
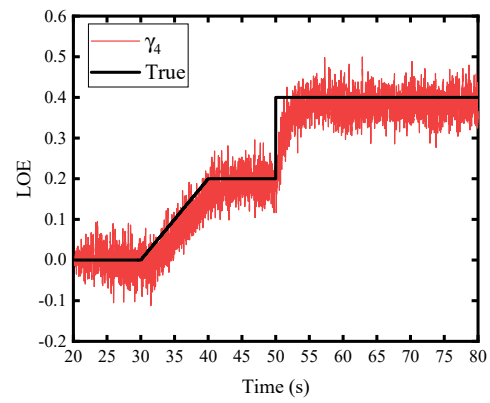


Figure 5. Cont.

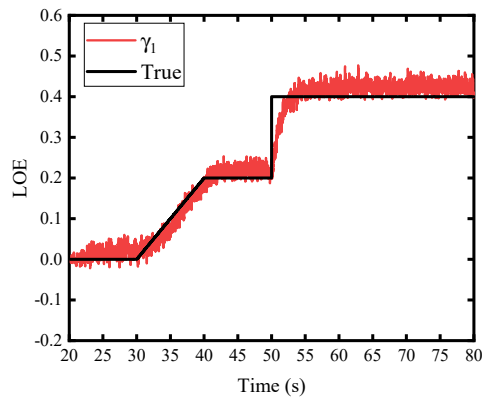


(c)

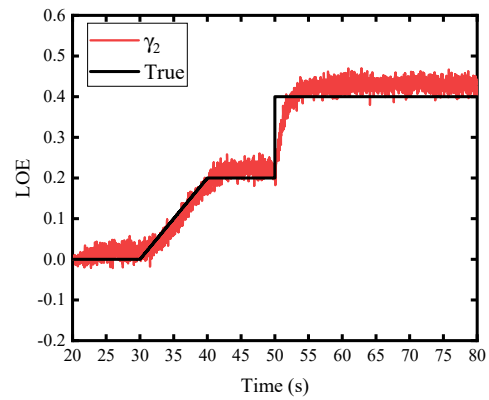


(d)

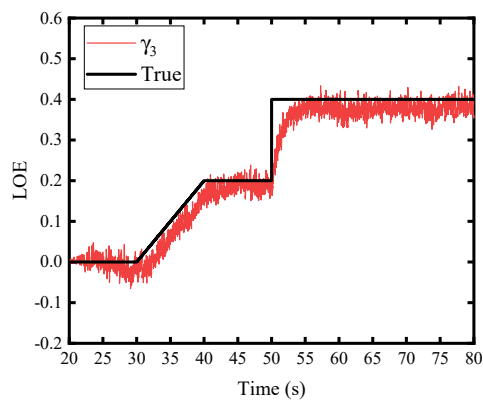
Figure 5. Simulation results using TSUKF when Q^Y matches the actual situation. (a) γ_1 ; (b) γ_2 ; (c) γ_3 ; (d) γ_4 .



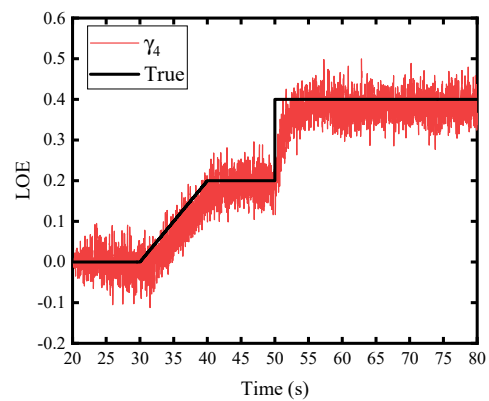
(a)



(b)

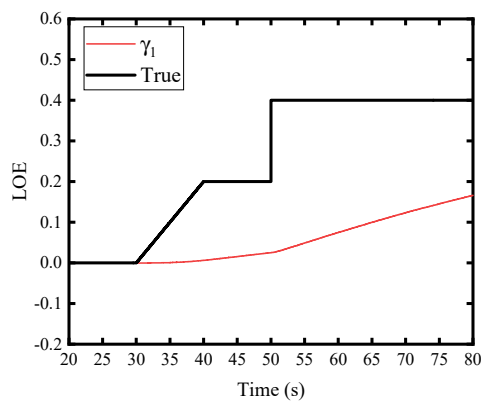


(c)

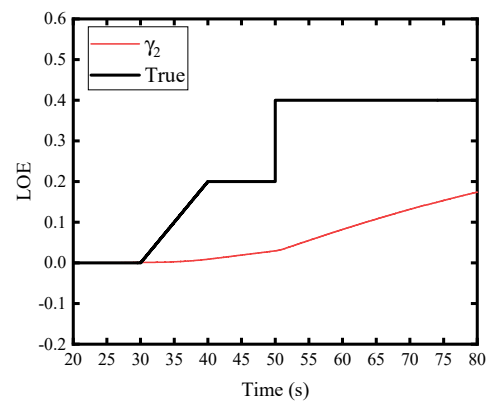


(d)

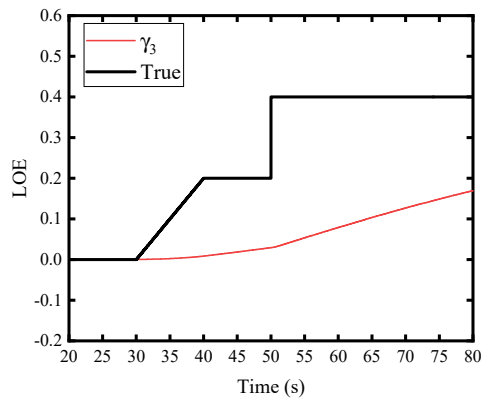
Figure 6. Simulation results using ATSUKF when Q^Y matches the actual situation. (a) γ_1 ; (b) γ_2 ; (c) γ_3 ; (d) γ_4 .



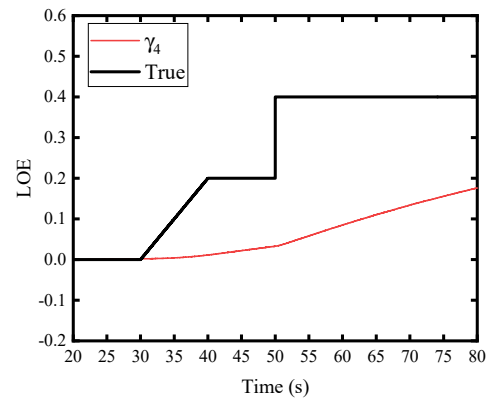
(a)



(b)

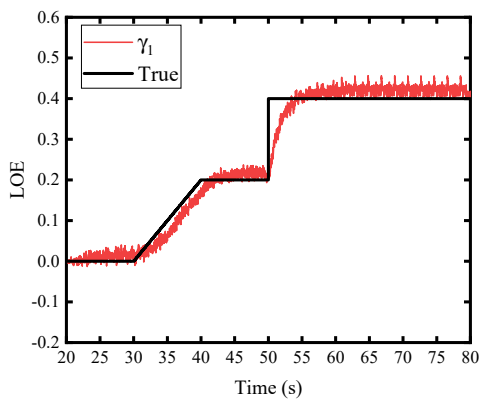


(c)

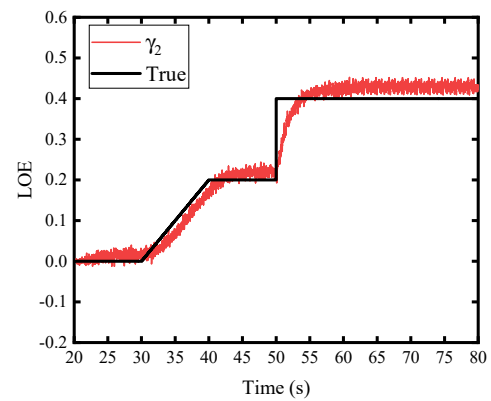


(d)

Figure 7. Simulation results using TSUKF when Q^Y mismatch the actual situation. (a) γ_1 ; (b) γ_2 ; (c) γ_3 ; (d) γ_4 .



(a)



(b)

Figure 8. Cont.

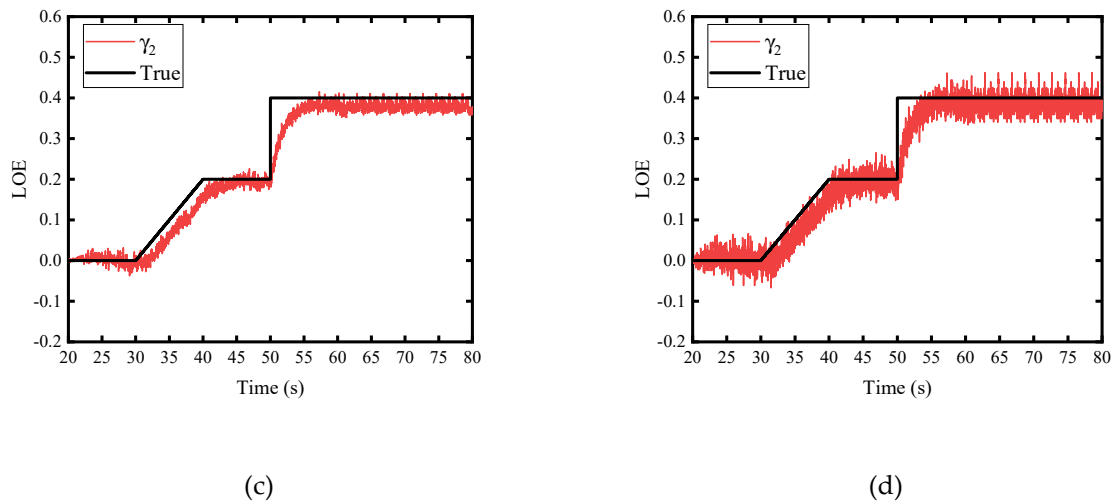


Figure 8. Simulation results using ATSUKF when Q^Y mismatches the actual situation. (a) γ_1 ; (b) γ_2 ; (c) γ_3 ; (d) γ_4 .

According to Figures 5–8, the LOE evaluation performance of the ATSUKF algorithm is better in the case of control efficiency loss of several motors. When the random model covariance matrix matches the actual covariance matrix, the TSUKF algorithm has higher evaluation accuracy and better stability than the ATSUKF algorithm. However, when the covariance matrix of the random walk model does not match the actual covariance matrix, the TSUKF algorithm cannot track the LOE factor state well, and the stability of the algorithm is weakened. The ATSUKF algorithm can still maintain the prediction accuracy of the random walk model when the covariance matrix is matched and has better robustness.

This section considers the matching relationship between the covariance matrix of the random model and the actual value and designs numerical simulations for single-motor and multi-motor LOE losses respectively to verify the TSUKF and ATSUKF algorithm. The results show that the ATSUKF algorithm is more robust to the initial value of the random walk model covariance than the TSUKF algorithm and has better performance. The random model covariance matrix in the TSUKF algorithm is a constant value matrix with an initial value given by experience, while the random model covariance matrix in the ATSUKF algorithm is a value change matrix obtained by covariance matching.

The dynamic characteristics of actuator degradation are unpredictable. Modeling the degradation as a random model with an unknown covariance matrix can better reflect the dynamic characteristics of the actuator's health state. Since the degeneration process of the actuator is usually slow in actual use, the covariance matrix usually takes a small value. When the actuator is degraded severely, the covariance matrix of TSUKF is difficult to adapt to the actual change of the health state of the actuator, and the accuracy of the algorithm decreases; while the ATSUKF algorithm will adaptively adjust the value of the diagonal elements according to the health state of the actuator. Compared with TSUKF, the ATSUKF algorithm can better match the actual system, so it has a better health status assessment effect. On the other hand, the covariance matrix of the random model is calculated online based on the filter divergence determination and covariance matching technology, so it has strong robustness to the initial value of the covariance matrix.

5. Conclusions

This paper proposes an actuator health assessment algorithm based on ATSUKF. The characteristics of the algorithm are as follows:

- This health assessment method only requires the control input signal and the attitude signal during flight without the real-time operation information of the actuator.

- The actuator health assessment can also be realized without fully understanding the actuator health state and the dynamic model of external interference.
- The nonlinear system model can be directly used in the filtering process through the traceless transformation, and the sensitivity to the changes in the actuator health state is enhanced by combining the filter divergence judgment and covariance matching technology.
- It is not only applicable to single actuator health assessments but also to multiple actuator health assessments.
- It is not only applicable to quad-rotor UAVs but also to other multi-rotor UAVs.

The simulations prove that the ATSUKF algorithm can reflect the dynamic characteristics of actuator health better than the TSUKF algorithm, and has better robustness and performance for the initial value of covariance. However, the calculation cost of ATSUKF is higher than that of TSUKF. In the next work, the iteration optimization of the ATSUKF algorithm will be realized by combining the actual UAV data.

Author Contributions: Conceptualization, M.Z. and G.L.; methodology, Z.Z.; software, S.Q.; validation, C.X., S.Q. and M.Z.; formal analysis, Z.Z.; investigation, C.X.; resources, G.L.; data curation, Z.Z.; writing—original draft preparation, Z.Z.; writing—review and editing, M.Z. All authors have read and agreed to the published version of the manuscript.

Funding: This research received no external funding.

Data Availability Statement: The data presented in this study are available on request from the corresponding author.

Conflicts of Interest: The authors declare no conflict of interest.

References

1. Hussein, H.; Benjamin, L.; Isabelle, F.; Clovis, F. Data Fusion Fault Tolerant Strategy for a Quadrotor UAV under Sensors and Software Faults. *ISA Trans.* **2022**, *1*, 7. [\[CrossRef\]](#)
2. Alemayehu, T.S.; Kim, J.H.; Yoon, W. Fault-Tolerant UAV Data Acquisition Schemes. *Wirel. Pers. Commun.* **2020**, *114*, 1669–1685. [\[CrossRef\]](#)
3. Igleis, E.; Horri, N.; Dahia, K.; Brusey, J.; Piet-Lahanier, H. Nonlinear Estimation of Sensor Faults With Unknown Dynamics for a Fixed Wing Unmanned Aerial Vehicle. In Proceedings of the 2021 International Conference on Unmanned Aircraft Systems (ICUAS), Athènes, Grèce, 19 July 2021. [\[CrossRef\]](#)
4. Igleis, E.; Horri, N.; Dahia, K.; Brusey, J.; Piet-Lahanier, H. Simultaneous Actuator and Sensor Faults Estimation for Aircraft Using a Jump-Markov Regularized Particle Filter. In Proceedings of the 2021 IEEE International Conference on Prognostics and Health Management (ICPHM), Détroit, MI, USA, 7–9 June 2021. [\[CrossRef\]](#)
5. Ducard, G. The SMAC Fault Detection and Isolation Scheme: Discussions, improvements, and application to a UAV. In Proceedings of the 2013 Conference on Control and Fault-Tolerant Systems (SysTol), Nice, France, 9–11 October 2013; pp. 480–485. [\[CrossRef\]](#)
6. Ren, X.L. Observer Design for Actuator Failure of a Quadrotor. *IEEE Access* **2020**, *8*, 152742–152750. [\[CrossRef\]](#)
7. Patton, R.J. Robust model-based fault diagnosis: The state of the art. *IFAC Proc. Vol.* **1994**, *27*, 1–24. [\[CrossRef\]](#)
8. Savkin, A.V.; Petersen, I.R. Model validation for robust control of uncertain systems with an integral quadratic constraint. *Automatica* **1996**, *32*, 603–606. [\[CrossRef\]](#)
9. Friedland, B. Treatment of bias in recursive filtering. *IEEE Trans. Autom. Control* **1969**, *14*, 359–367. [\[CrossRef\]](#)
10. Gillijns, S.; Moor, B.D. Brief paper: Unbiased minimum-variance input and state estimation for linear discrete-time systems. *Automatica* **2007**, *43*, 111–116. [\[CrossRef\]](#)
11. Steven, G.; Moor, B.D. Unbiased minimum-variance input and state estimation for linear discrete-time systems with direct feedthrough. *Automatica* **2007**, *43*, 934–937. [\[CrossRef\]](#)
12. Simon, D.J. *Optimal State Estimation: Kalman, H ∞ , and Nonlinear Approaches*; Wiley-Interscience: New York, NY, USA, 2006.
13. Zhang, H.; Gao, Q.; Pan, F. An Online Fault Diagnosis Method for Actuators of Quadrotor UAV with Novel Configuration Based on IMM. In Proceedings of the 2020 Chinese Automation Congress (CAC), Shanghai, China, 6–8 November 2020. [\[CrossRef\]](#)
14. Zhong, Y.; Zhang, Y.; Zhang, W.; Zuo, J.; Zhan, H. Robust Actuator Fault Detection and Diagnosis for a Quadrotor UAV with external Disturbances. *IEEE Access* **2018**, *6*, 1. [\[CrossRef\]](#)
15. Gao, J.; Zhang, Q.; Chen, J. EKF-Based Actuator Fault Detection and Diagnosis Method for Tilt-Rotor Unmanned Aerial Vehicles. *Math. Probl. Eng.* **2020**, *1*, 1–12. [\[CrossRef\]](#)
16. Qi, J.T.; Jiang, Z.; Zhao, X.G. Adaptive UKF and Its Application in Fault Tolerant Control of Rotorcraft UAV. In Proceedings of the AIAA Guidance, Navigation and Control Conference and Exhibit, Hilton Head, SC, USA, 20–23 August 2007. [\[CrossRef\]](#)

17. Bouabdallah, S.; Pierpaolo, M.; Roland, S. Design and control of an indoor micro quadrotor. In Proceedings of the IEEE International Conference on Robotics and Automation, New Orleans, LA, USA, 26 April–1 May 2004. [[CrossRef](#)]
18. Zio, E. Reliability engineering: Old problems and new challenges. *Reliab. Eng. Syst. Saf.* **2009**, *94*, 125–141. [[CrossRef](#)]
19. Botchev, V. Kalman filtering: With real-time applications. *Comput. Rev.* **2020**, *51*, 404–405. [[CrossRef](#)]
20. He, Q.; Zhang, W.; Liu, X.; Liu, J. Information Fusion and Reconstruction of Key Sensors in a Flight Control System in Constant Wind Field based on Two Stage EKF. In Proceedings of the 2016 IEEE Chinese Guidance, Navigation and Control Conference (CGNCC), Nanjing, China, 12 August 2016. [[CrossRef](#)]
21. Julier, S.J. Unscented Filtering and Nonlinear Estimation. *Proc. IEEE* **2004**, *92*, 401–422. [[CrossRef](#)]
22. Chen, X.; Sun, R.; Wang, F.; Song, D.; Jiang, W. Two-stage unscented kalman filter algorithm for fault estimation in spacecraft attitude control system. *IET Control. Theory Appl.* **2018**, *12*, 1781–1791. [[CrossRef](#)]
23. Li, W.; Wang, C.W. Research on life prediction and life extension method of feedback control system under actuator degradation. *IEEE Access* **2020**, *4*, 67.
24. Sriyanand, H. A simple method for the control of divergence in Kalman-filter algorithms. *Int. J. Control* **1972**, *16*, 1101–1106. [[CrossRef](#)]
25. Yang, Y.; Gao, W. A new learning statistic for adaptive filter based on predicted residuals. *Prog. Nat. Sci.* **2006**, *16*, 833–837. [[CrossRef](#)]
26. Quan, Q.; Dai, X.; Wang, S. *Multicopter Design and Control Practice: A Series Experiments Based on MATLAB and Pixhawk*; Springer Nature: Singapore, 2020.

Disclaimer/Publisher’s Note: The statements, opinions and data contained in all publications are solely those of the individual author(s) and contributor(s) and not of MDPI and/or the editor(s). MDPI and/or the editor(s) disclaim responsibility for any injury to people or property resulting from any ideas, methods, instructions or products referred to in the content.